

Noise figure improvement and quantum information tapping in a fiber optical parametric amplifier with correlated quantum fields

Xueshi Guo¹, Nannan Liu¹, Xiaoying Li^{1,*}, Yuhong Liu¹, Z. Y. Ou^{2,†}

¹ College of Precision Instrument and Opto-electronics Engineering, Tianjin University,

Key Laboratory of Optoelectronics Information Technology, Ministry of Education, Tianjin, 300072, P. R. China

² Department of Physics, Indiana University-Purdue University Indianapolis, Indianapolis, IN 46202, USA

E-mail: *xiaoyingli@tju.edu.cn †zou@iupui.edu

Abstract. We experimentally demonstrate an improvement of 0.7 ± 0.1 dB in the noise figure in a low noise fiber-optical parametric amplifier (FOPA) with the injection of correlated quantum fields generated from spontaneous four-wave mixing in fibers. The noise performance of the amplifier is characterized with homodyne detectors. The experimental result shows that the noise levels in the two output ports (signal and idler) of the amplifier are both 1.0 ± 0.1 dB lower than a regular FOPA with vacuum at the unused input port. In addition, we demonstrate the scheme can be used as a quantum information tap with a combined information transfer efficiency (signal and tap) as $T_{sig} + T_{tap} = 1.47 \pm 0.2$, which is larger than the classical limit of 1. This low noise FOPA can be applied to the low noise amplification in the measurement of weak signals.

1. Introduction

Quantum information is notoriously prone to the influence of unwanted noise. Thus, amplification of a quantum signal without adding in extra noise is of great interest in a wide area in both fundamental study such as quantum measurement of weak signals and practical applications such as quantum communication and quantum information processing. In general, the principles of quantum mechanics prevent us from noiseless amplification of a signal in an arbitrary quantum state [1, 2, 3]. But for a set of specific states, noiseless amplification is possible. Indeed, noiseless quantum amplification was achieved in a phase-sensitive parametric amplifier in which one quadrature-phase amplitudes of an optical field is amplified noiselessly while the other orthogonal one is de-amplified [4, 5]. Such a scheme was recently applied in an optical network to improve the noise figure in the amplification of classical signals [6]. However, phase-sensitive

amplifiers are not widely used because of the technological complications involved to stabilize the phase-dependent gain, which may introduce extra noise in the amplified signal through phase fluctuations.

On the other hand, the commonly used phase-insensitive amplifiers such as erbium-doped fiber amplifiers (EDFAs) [7] and Raman amplifiers [8], when operated with internal modes unattended, are known to add quantum noise to the amplified signal, leading to a noise figure (NF) of 3 dB at large gain [1, 2, 3]. The added extra noise are from the vacuum noise in the unattended internal degrees of freedom of the amplifier. This extra noise is detrimental to the amplification of a quantum signal. Thus, squeezed states were used to reduce the extra noise [9, 10]. Recently, a phase-insensitive amplification scheme with quantum sources of correlated noise [11] was realized in a demonstration-of-principle experiment with a parametric amplifier in an atomic system [12]. In this scheme, the internal noise of the amplifier was cancelled through quantum interference between quantum sources of correlated noise, reducing significantly the quantum noise in amplification. Here, we apply the same idea to a fiber optical parametric amplifier (FOPA), and our result shows that the noise levels in the two output ports (signal and idler) of the FOPA are both about 1 dB lower than a regular FOPA with vacuum at the unused input port. Our FOPA is realized by utilizing the four-wave mixing (FWM) process in optical fiber to achieve parametric amplification, and all the optical fields involved in the FWM process (including the pump, signal and idler) are in the 1550 nm telecom band. Therefore, our system is suitable for the practical implementation of quantum information processing tasks.

In this paper, in addition to the noise reduction, we are more interested in the change of NF of the FOPA due to extra noise in the amplification process. To mimic a practical application as close as possible, we generate the input signal by modulating a weak probe coupled either to vacuum (regular situation) or to one of the correlated quantum fields. The experimental results demonstrate that an improvement of 0.7 dB in the NF is achieved when the FOPA is operating in the latter case.

Additionally, as is well known, optical information tapping with a linear beam splitter will always introduce vacuum noise through the unused port, leading to an overall information transfer efficiency less than one [13], but one can achieve an overall information transfer efficiency larger than one if the vacuum noise from the unused port can be squeezed [13, 14, 15, 16, 17], which leads to quantum information cloning. Since the low noise FOPA with quantum correlated input fields has two output ports (signal and idler), the device can be viewed as a information splitter. Hence, we will investigate the overall information transfer efficiency of the FOPA and compare it to the classical limit of one as well.

2. The Principle of the Experiment

Figure 1(a) shows the diagram of a regular FOPA, which has two inputs and two outputs, traditionally named "signal" and "idler", respectively, and the injection of the unused

idler input port is vacuum. Fig. 1(b) shows the conceptual diagram of our low noise FOPA using correlated source as input, which consist of two FOPAs. The first one (FOPA1) acts as a correlated quantum fields generator, which, when operated without any coherent input and therefore with only vacuum input, produces two highly correlated quantum fields, dubbed also as signal and idler beams by convention [18]. These two correlated quantum fields each by themselves are in a thermal state or amplified vacuum state and do not have a coherent component. Since we need to have a coherent part to fulfill the task of encoding information, we then combine a bright coherent state $|\alpha\rangle$ with one (signal field) of the correlated fields generated from FOPA1 at a beam splitter (BS). After propagating through a test sample, the combined field which functions as a probe is sent to the signal input port of the second FOPA (FOPA2), which is the amplifier we are interested in and will investigate throughout this paper. To study the amplifier with the correlated noise input, we will inject the other one (idler field) of the correlated fields from FOPA1 into the idler input port of FOPA2. The information obtained by passing the probe through the sample is amplified and comes out at both the signal and idler output ports of FOPA2. The noise level of FOPA2 is governed by the correlated fields generated from FOPA1 when the reflectance (transmittance) of the BS satisfies the relation $r \approx 1$ ($t \ll 1$), but the signal level, which contains the information of the sample, is dominated by the intensity of coherent state $|\alpha\rangle$ if the amplitude of the input signal $|\alpha\rangle$ is large enough ($|\alpha|^2 t^2 \gg 1$).

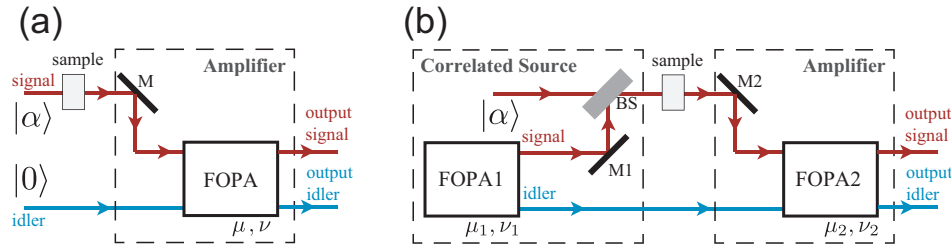


Figure 1. The conceptual diagram of parametric amplifier with its internal mode (idler mode) (a) in vacuum and (b) correlated with the input signal mode, respectively. FOPA1 with vacuum input generates signal and idler fields with correlated noise via spontaneous FWM. The probe light of FOPA2 is obtained by combining the signal field out of FOPA1 with a coherent state $|\alpha\rangle$ at BS. The noise level of FOPA2 can be reduced when the idler field of FOPA1 is launched into FOPA2 as well. Both the signal and idler outputs of FOPA2 contain the information of the sample with NF better than a regular FOPA in plot (a). BS, beam splitter with near unity reflection coefficient; M1, M2: high reflection mirrors.

Next, we briefly analyze the noise performance and signal to noise ratio (SNR) for the amplification scheme in Fig.1(b) and compare the result with that for scheme in Fig.1(a). Assuming the signal and idler input modes of a FWM based amplifier are described by the operators \hat{a}_s and \hat{a}_i , respectively, the operators \hat{b}_s and \hat{b}_i of the signal and idler output modes can be written as [19]:

$$\hat{b}_{s(i)} = \mu \hat{a}_{s(i)} + e^{i\theta_p} \nu \hat{a}_{i(s)}^\dagger, \quad (1)$$

where $\mu = \cosh g$ and $\nu = \sinh g$ are amplitude gain of the amplifier, and $g > 0$ represents the nonlinear coupling coefficient of FWM; θ_p is the phase of the pump.

For a given mode \hat{a} , the quadrature amplitude/phase operator, defined as $\hat{X}(\theta) = \frac{1}{\sqrt{2}}(e^{-i\theta}\hat{a} + e^{i\theta}\hat{a}^\dagger)$, is more often used to convey information since it can be directly detected by a homodyne detector. So, the input signal of FOPA2 is expressed as

$$\langle \hat{X}_{in}(\theta) \rangle = t(\alpha e^{-i\theta} + \alpha^* e^{i\theta}) \quad (2)$$

According to Eq.(1), the signal and idler outputs, $\hat{X}_s(\theta)$ and $\hat{X}_i(\theta)$, can be expressed as:

$$\langle \hat{X}_s(\theta) \rangle = \mu_2 t(\alpha e^{-i\theta} + \alpha^* e^{i\theta}) \quad (3)$$

$$\langle \hat{X}_i(\theta) \rangle = \nu_2 t[\alpha e^{-i(\theta+\theta_{p2})} + \alpha^* e^{i(\theta+\theta_{p2})}], \quad (4)$$

when the phase of the pumps of FOPA1 and FOPA2 (see Fig.1(b)) are set to be θ_{p1} and θ_{p2} , respectively, where μ_2 and ν_2 are amplitude gain of FOPA2. Note that the quadrature angle of the signal output field remains the same as the coherent state $|\alpha\rangle$, but the quadrature angle of the idler output field is shifted by the amount of θ_{p2} , which is originated from the FWM process in FOPA2.

Since the noise level of the input of FOPA2 is determined by the correlated noise source (FOPA1), the input signal of the bright coherent state $|\alpha\rangle$ can be ignored during the process of analyzing the noise performance. At the output port of FOPA2, the operator represents the noise of the quadrature amplitude/phase of signal (idler) $\hat{X}_{s(i)}^n(\theta)$ can be obtained by using Eq.(1) twice :

$$\begin{aligned} \hat{X}_{s(i)}^n(\theta) &= |\mu_1\mu_2 + e^{-i(\theta_{p2}-\theta_{p1})}\nu_1\nu_2|\hat{X}_{s0(i0)}(\theta_s) \\ &\quad + |e^{-i\theta_{p1}}\nu_1\mu_2 + e^{-i\theta_{p2}}\mu_1\nu_2|\hat{X}_{i0(s0)}(\theta_i), \end{aligned} \quad (5)$$

where μ_1 and ν_1 are the amplitude gain of FOPA1, $\hat{X}_{s0(i0)}(\theta_{s(i)})$ denotes the noise at the signal (idler) input port of FOPA1, and $\theta_s = \theta + \arg(\mu_1\mu_2 + e^{-i(\theta_{p2}-\theta_{p1})}\nu_1\nu_2)$ and $\theta_i = \theta + \arg(e^{-i\theta_{p1}}\nu_1\mu_2 + e^{-i\theta_{p2}}\mu_1\nu_2)$ are the phase of the quadrature components shifted by the amplification process. For FOPA1 with vacuum as the input, the variance of the noise operator satisfies $\langle \Delta^2 \hat{X}_{s0(i0)}(\theta) \rangle \equiv \langle \hat{X}_{s0(i0)}^2(\theta) \rangle - \langle \hat{X}_{s0(i0)}(\theta) \rangle^2 = 1$ for an arbitrary value of θ . Therefore, the noise variance at the signal and idler outputs of FOPA2 can be deduced:

$$\begin{aligned} \langle \Delta^2 \hat{X}_s^n(\theta) \rangle &= \langle \Delta^2 \hat{X}_i^n(\theta) \rangle = \mu_1^2\mu_2^2 + \nu_1^2\nu_2^2 + \mu_1^2\nu_2^2 + \nu_1^2\mu_2^2 \\ &\quad - 4\mu_1\mu_2\nu_1\nu_2 \cos(\theta_{p2} - \theta_{p1}). \end{aligned} \quad (6)$$

Equation (3) shows that the average value of signal amplified by FOPA2 does not depend on the phase of pumps θ_{p1} and θ_{p2} , indicating FOPA2 is a phase insensitive amplifier. However, Eq.(6) reveals that the noise of its amplified output ports changes with the phases of the pumps. Under the condition $\theta_{p2} - \theta_{p1} = \pi$, the noise variance is minimized and can be written as:

$$\begin{aligned} \langle \Delta^2 \hat{X}_s^n(\theta) \rangle &= \langle \Delta^2 \hat{X}_i^n(\theta) \rangle = \mu_1^2\mu_2^2 + \nu_1^2\nu_2^2 + \mu_1^2\nu_2^2 + \nu_1^2\mu_2^2 - 4\mu_1\mu_2\nu_1\nu_2 \\ &= 1 + 2(\mu_1\nu_2 - \mu_2\nu_1)^2, \end{aligned} \quad (7)$$

in which the relations of the amplitude gain $\mu_1^2 - \nu_1^2 = 1$ and $\mu_2^2 - \nu_2^2 = 1$ are applied. In this situation, the SNRs for the signal and idler outputs of FOPA2 with correlated noise input $R_{s,i}^c$ are

$$\begin{aligned} R_s^c &= \frac{\langle \hat{X}_s(\theta) \rangle^2}{\langle \Delta^2 \hat{X}_s^n(\theta) \rangle} = \frac{\mu_2^2 t^2 (\alpha e^{-i\theta} + \alpha^* e^{i\theta})^2}{1 + 2(\mu_1 \nu_2 - \mu_2 \nu_1)^2} \\ R_i^c &= \frac{\langle \hat{X}_i(\theta) \rangle^2}{\langle \Delta^2 \hat{X}_i^n(\theta) \rangle} = \frac{\nu_2^2 t^2 (\alpha e^{-i(\theta+\theta_p)} + \alpha^* e^{i(\theta+\theta_p)})^2}{1 + 2(\mu_1 \nu_2 - \mu_2 \nu_1)^2}. \end{aligned} \quad (8)$$

Note that without the injection of correlated quantum fields, i.e., $\mu_1 = 1, \nu_1 = 0$ (this corresponds to the scheme in Fig.1(a)), the SNRs at the signal and idler outputs of the amplifier are

$$\begin{aligned} R_s^v &= \frac{\mu_2^2 t^2 (\alpha e^{-i\theta} + \alpha^* e^{i\theta})^2}{\mu_2^2 + \nu_2^2} \\ R_i^v &= \frac{\nu_2^2 t^2 (\alpha e^{-i\theta} + \alpha^* e^{i\theta})^2}{\mu_2^2 + \nu_2^2}. \end{aligned} \quad (9)$$

Hence, the improvement in SNR due to the using of the correlated quantum field is

$$\frac{R_s^c}{R_s^v} = \frac{R_i^c}{R_i^v} = \frac{\mu_2^2 + \nu_2^2}{1 + 2(\mu_1 \nu_2 - \mu_2 \nu_1)^2}. \quad (10)$$

From Eq. (10), one sees that $\frac{R_s^c}{R_s^v}$ and $\frac{R_i^c}{R_i^v}$ reaches the maximum $\mu_2^2 + \nu_2^2$ under the condition $\mu_1 = \mu_2, \nu_1 = \nu_2$. In this situation, FOPA2 is a reverse process of FOPA1. The noise level at the output of FOPA2 is simply $\langle \Delta^2 \hat{X}_s^n(\theta) \rangle = 1$ (see Eq.(6)), which means that the output noise level of FOPA2 remains the same as the vacuum state even with amplification. On the other hand, for the case of $\mu_1 = 1, \nu_1 = 0$, i.e., without using the correlated quantum field, the noise level of FOPA2 will be $\langle \Delta^2 \hat{X}_s^n(\theta) \rangle = \mu_2^2 + \nu_2^2$. The noise reduction from $\mu_2^2 + \nu_2^2$ to 1, which results in the improvement of SNR, is due to a quantum interference effect for noise cancellation [12].

The above analysis indicates that comparing with a regular amplifier (Fig.1(a)), the amplification scheme in Fig.1(b) obviously possesses low noise feature. In reality, the noise reduction effect is limited by the optical loss between FOPA1 and FOPA2 [20] and by other technical noise, but Fig.1(b) is still a promising low noise amplification scheme, which is suitable for amplifying of the measurement signals obtained by passing a weak probe light through a near transparent sample.

In addition to the noise level, we also study the NF, which is defined as the ratio between the SNRs at the input and output ports and is often used for characterizing the performance of an amplifier. We first analyze the NF under the condition of $\mu_1 = 1, \nu_1 = 0$. In this case, FOPA2 is equivalent to a regular FOPA in Fig.1(a). For the input signal in Eq. (2), the SNR of input signal is simply $R_{in}^v = t^2 (\alpha e^{-i\theta} + \alpha^* e^{i\theta})^2$ because the noise is the shot noise or vacuum noise. According to expression of SNR in Eq. (9), we have the NFs at the signal and idler output ports:

$$N_s^v \equiv \frac{R_{in}^v}{R_s^v} = \frac{\nu_2^2}{\mu_2^2} + 1, \quad (11)$$

and

$$N_i^v \equiv \frac{R_{in}^v}{R_i^v} = \frac{\mu_2^2}{\nu_2^2} + 1. \quad (12)$$

Eqs. (11) and (12) clearly show $N_{s(i)}^v \rightarrow 2$ for $\mu_2 \rightarrow \infty$, which is the famous 3 dB NF limit of a regular phase insensitive amplifier. We then analyze the NF under the condition of $\nu_1 > 0$, which means FOPA2 has correlated noise inputs. In this case, the average of input signal is still described by Eq. (2), but the noise becomes $\langle \Delta^2 \hat{X}_{in}^n \rangle = \langle (\Delta \hat{X}_s^n - \lambda \Delta \hat{X}_i^n)^2 \rangle$ [11]. Moreover, the minimized noise level of $\langle \Delta^2 \hat{X}_{in}^n \rangle = 1/(\mu_1^2 + \nu_1^2)$ can be obtained under the condition $\lambda = \nu_1/\mu_1$, and the corresponding SNR at the input port is $R_{in}^c = t^2(\alpha e^{-i\theta} + \alpha^* e^{i\theta})^2(\mu_1^2 + \nu_1^2)$. According to expression of SNR in Eq. (8), we obtain the NFs at the signal and idler output ports:

$$N_s^c \equiv \frac{R_{in}^c}{R_s^c} = [1 + 2(\mu_1\nu_2 - \mu_2\nu_1)^2] \frac{\mu_1^2 + \nu_1^2}{\mu_2^2}, \quad (13)$$

$$N_i^c \equiv \frac{R_{in}^c}{R_i^c} = [1 + 2(\mu_1\nu_2 - \mu_2\nu_1)^2] \frac{\mu_1^2 + \nu_1^2}{\nu_2^2}. \quad (14)$$

It is straightforward to deduce that the minimized values of $N_s^c = 1$ and $N_i^c = \mu_2^2/\nu_2^2$ can be realized under the condition $\mu_2 = \mu_1^2 + \nu_1^2$, which indicates that a noiseless amplification characterized by the value of NF $N_s^c = 1$ is achievable. Using the expressions of NF in Eqs. (11)-(14), we have

$$\frac{N_s^c}{N_s^v} = \frac{N_i^c}{N_i^v} = \frac{\mu_2^2}{\mu_2^2 + \nu_2^2}, \quad (15)$$

which shows that NF at both the signal and idler outputs can be improved by using FOPA2 with the injection of quantum correlated fields.

Since the information of the input signal are transferred to both the signal and idler outputs during the amplification process of FWM, we analyze the information transfer coefficients of the FOPA2 as well. According to the definition of transfer coefficient at signal and idler (tap) output ports

$$T_{sig} \equiv \frac{R_s^c}{R_{in}^c} = \frac{1}{N_s^c}, \quad T_{tap} \equiv \frac{R_i^c}{R_{in}^c} = \frac{1}{N_i^c}, \quad (16)$$

and Eqs.(13) and (14), we obtain the maximum values for T_{sig} and T_{tap}

$$T_{sig} + T_{tap} = 1 + \nu_2^2/\mu_2^2 \rightarrow 2 \quad \text{for } \mu_2 \rightarrow \infty, \quad (17)$$

when the condition for realizing the optimized NF $\mu_2 = \mu_1^2 + \nu_1^2$ is satisfied. Thus, FOPA2 with the injection of quantum correlated fields, whose two outputs are amplified copies of the input, can perform the function of a quantum information tap to split an input signal into two copies without adding noise. Although this is similar to the quantum clone amplifier in Ref. [14], here we achieve the same with a phase-insensitive amplifier instead of a phase-sensitive one.

3. Experiment:

3.1. Experimental setup

Our experimental setup is shown in Fig. 2(a). The nonlinear media of the source of correlated fields (FOPA1) and low noise amplifier (FOPA2) are two pieces of dispersion shifted fiber (DSF1 and DSF2). The dispersion properties of the two DSFs are identical, and the length of each DSF with zero dispersion wavelength of about 1550 nm is about 300 m. The pumps P1 and P2 have the same central wavelength 1552.5 nm, which is in the anomalous dispersion region of DSF1/DSF2, so the phase matching condition of FWM with broad gain bandwidth is satisfied in both DSF1 and DSF2. The quantum correlated signal and idler fields are generated by spontaneous FWM in DSF1 and separated by a coarse wavelength division multiplexer (CWDM1), whose four-channels are centering at 1511, 1531, 1551, and 1571 nm, respectively, and the one-dB bandwidth of each channel is about 16 nm. FOPA2 consists of two CWDMs and DSF2. The signal field out of DSF1 is combined with a pulsed coherent input $|\alpha\rangle$ at a 95:5 fiber coupler (FC) to form the probe light. The task of encoding information being amplified by FOPA2 is realized by passing the probe through an electro-optics modulator (EOM). The probe carrying the information encoded on EOM, the idler field out of DSF1, and the pump P2, which are centering at 1569, 1552.5 and 1534 nm, respectively, are coupled into the DSF2 by CWDM2. The noise level of FOPA2 is sensitive to the phase difference of the pumps P1 and P2 (see Eq. (6)), so we control the phase of P2 by mounting a piezo-electronic transducer (PZT) on a high reflection mirror. The signal and idler outputs of FOPA2, separated by CWDM3, are respectively detected by the homodyne detection (HD) systems, HDs and HDi, whose local oscillators (LO) are labeled as LOs and LOi, respectively.

In order to obtain the pumps P1 and P2, the LO of each HD, and the coherent input $|\alpha\rangle$, we first disperse the 40 MHz train of 150-fs pulses center at 1560 nm from a mode-locked fiber laser with a grating and spectrally filter them to obtain three beams, whose central wavelengths (pulse durations) are 1569 (3), 1552.5 (4) and 1534 (3) nm (ps), respectively (see Fig. 2(b)). We then propagate the beam at 1552.5 nm through the FC3 (50:50) and amplify each output of FC3 by EDFA2 and EDFA3, respectively, to achieve the required power of the pumps. The output of EDFA2/EDFA3 is further cleaned up with a bandpass filter F2/F3 centering at 1552.5 nm and having a FWHM of 0.8 nm. To ensure the polarization and power adjustment of the pump P1/P2, the output of F2/F3 is then passed through a fiber polarization controller (FPC) FPC5/FPC6 and polarization beam splitter (PBS) PBS1/PBS2. The LOi is achieved by amplifying the beam at 1534 nm with EDFA1 and propagating through filter F1 (centered at 1534 nm with a FWHM of 1 nm). LOs is directly obtained by passing the beam at 1569 nm, with power of about 450 μ W, through the 90% port of FC4, while the coherent input $|\alpha\rangle$ is accordingly obtained at the 10% port of FC4.

For the realization of low noise amplifier, it is important to match the modes of all the optical fields involved in the FWM in FOPA2. We first match the modes of

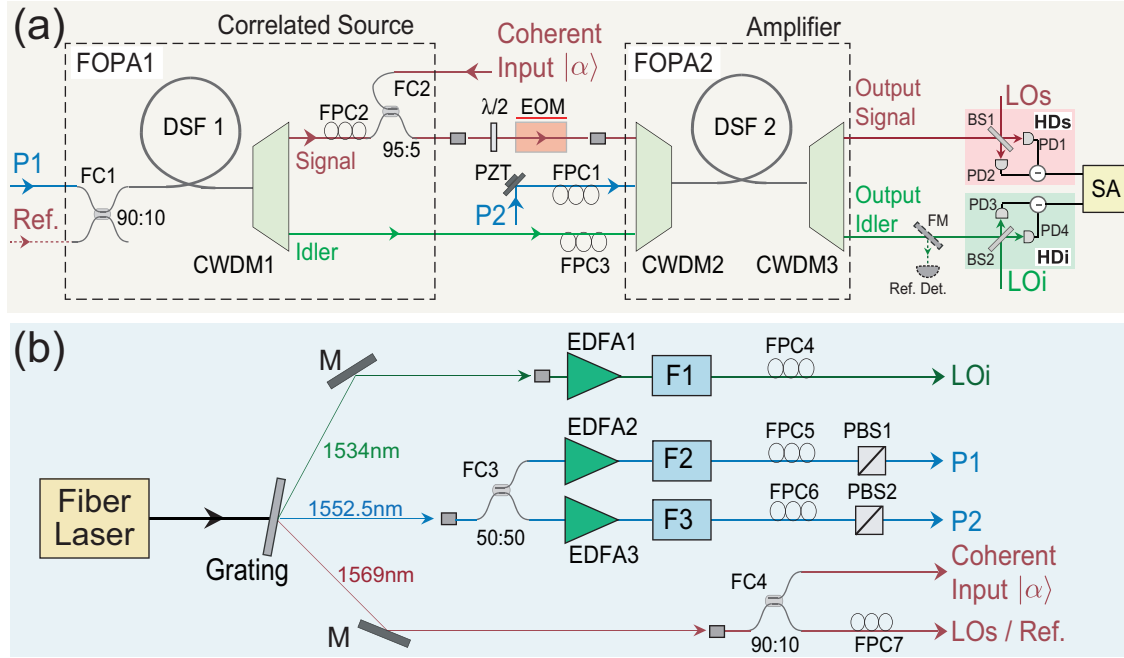


Figure 2. (a) Experimental setup of the low noise amplifier with correlated noise input. (b) The scheme for preparation of pulsed pumps (P1, P2), coherent state input signal, local oscillator (LOs, LOi) and reference signal (Ref.). DSF, dispersion shifted fiber; CWDM, coarse wavelength division multiplexer; FPC, fiber polarization controller; FC, fiber coupler; EOM, electro-optical modulator; HD, homodyne detection; SA, electronic spectrum analyzer; EDFA, erbium-doped fiber amplifier; F, filter; PBS, polarization beam splitters; FM, flip mirror; Ref. reference light; Ref. Det., reference detector.

the coherent input $|\alpha\rangle$ at the 5% port of FC2 and P2 by adjusting the optical paths to maximize their pulse overlap and tuning the polarization of P2 with FPC1 for efficient FWM in DSF2. We then work on matching the modes of the correlated signal and idler fields with that of P2 when a reference light (Ref., obtained by attenuating the LOs to about $2 \mu\text{W}$) is injected into DSF1 through the 10% port of FC1 but the input $|\alpha\rangle$ of FOPA2 is blocked. In this case, FWM in DSF1 is phase insensitive while that in DSF 2 is phase sensitive. After matching the modes of the injected reference light and P1 by adjusting their optical paths to maximize the pulse overlap and by tuning the polarization with FPC7 for efficient FWM in DSF1, we adjust optical paths and tuning polarization of signal and idler fields with FPC2 and FPC3 to match their modes with P2 in DSF2. In this process, the powers of both P1 and P2 are about 1.1 and 1.7 mW, the phase of P2 is scanned by sweeping the voltage of PZT, and the idler output port of FOPA2 is monitored by using a flip mirror (FM) to reflect the light and by using a reference detector (Ref. Det.) to measure the power. Fig. 3 shows the simultaneously recorded output of reference detector and the voltage of PZT. One sees that the power at the idler output periodically varies with the sweep of voltage, which is referred to as nonlinear interference fringe [21], and the nearly 100% interference visibility indicates the required mode matching in FOPA2 is achieved. Note that the reference light is only

Noise figure improvement and quantum information tapping in a fiber optical parametric amplifier with correlated inputs
 used for mode matching, it is blocked in the experiment presented hereinafter.

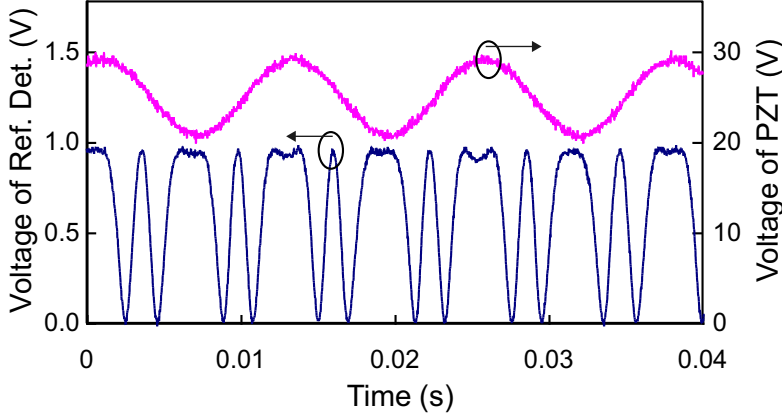


Figure 3. Variation of the power at the idler output port when the reference light is injected into DSF1 and the voltage of PZT is swept.

The performance of FOPA2 is investigated by measuring the variance of quadrature amplitude and phase at the signal/idler output under different experimental conditions. The measurement is carried out by using HDs/HDi, which is comprised of a 50:50 BS1/BS2 and two photodiodes (PD, ETX-500) with circuits same as those in Ref. [22]. During the measurement process, the required mode matching between the measured signal/idler output and LOs/LOi is achieved by adjusting the polarization of LOs/LOi with FPC7/FPC4, the power of LOs/LOi is about 0.4/2 mW, and the outputs of HDs/HDi is analyzed by an electronic spectrum analyzer (SA).

3.2. Noise reduction

We first study the noise performance of FOPA2. In the experiment, the coherent input $|\alpha\rangle$ is blocked. After characterizing the shot noise level (SNL) of HDs/HDi by blocking the pumps P1 and P2, we measure the noise level at signal/idler output port of FOPA2 when the powers of P1 and P2 are about 1.1 and 1.7 mW, respectively. At this power level of pumps, the parametric photon number gains of FOPA1 and FOPA2 are about 8 and 20, respectively [22]. Moreover, to illustrate the essentiality of the correlated inputs on the noise reduction, after measuring the noise of the signal/idler input by blocking both the idler/signal input and the pump P2, we measure the noise level of the FOPA2 by blocking the idler input port of FOPA2. Furthermore, to interpret the noise of FOPA2 with correlated inputs is lower than a regular FOPA with vacuum at the unused idler port, we also measure the noise at the signal/idler output by blocking the pump P1 ($\mu_1 = 1, \nu_1 = 0$).

Figures 4(a) and 4(b) show the noise levels measured at the signal and idler output ports, respectively. In each figure, trace (i) is the SNL of the homodyne detection system. Traces (ii) and (iii) are the noise level of FOPA2 with correlated inputs, which are obtained by scanning the phase of P2 and setting the phase to P2 to achieve the

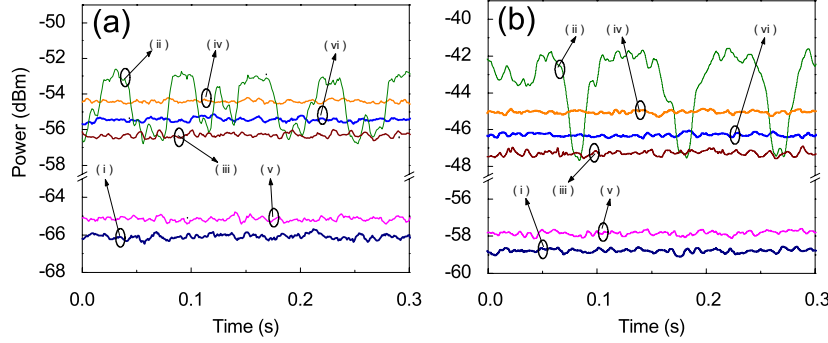


Figure 4. The noise levels measured at (a) signal and (b) idler output ports under different conditions. Trace (i) is the SNL of the homodyne detection system; traces (ii) and (iii) are the noise level of FOPA2 with correlated inputs, obtained by scanning the phase of P2 and setting the phase of P2 to achieve the best noise cancellation, respectively; trace (iv) is noise level of FOPA2 obtained by blocking the idler/signal field out of DSF1; trace (v) is the noise level of the input signal/idler of FOPA2; trace (vi) is the noise level of a regular FOPA with vacuum at the idler port. In the measurement, trace (i) is obtained by blocking the pumps of both DSF1 and DSF2; traces (ii)-(iv) are obtained for P1 and P2 with powers of 1.1 and 1.7 mW, respectively; trace (v) is obtained for P1 and P2 with powers of 1.1 and 0 mW, respectively; trace (vi) is obtained for P1 and P2 with powers of 0 and 1.7 mW, respectively. In the measurement, SA is set to zero span at 2 MHz and the noise of the homodyne detection system itself is subtracted.

lowest noise, respectively. It is obvious that the results agree with Eq. (6): the noise level varies with the relative phase difference between P1 and P2, and the best noise cancellation can be achieved by properly setting the phase of P2. Trace (iv) is noise level of FOPA2 obtained by blocking the idler/signal field out of DSF1 and using the signal/idler field out of DSF1 as the input. Comparing trace (iv) with traces (ii) and (iii), one sees that trace (iv) is lower than the highest point of trace (ii) but is higher than trace (iii). The comparison indicates that the idler field, correlated with the input of signal, plays an important role in reducing the noise of FOPA2. Moreover, comparing minimized noise level of FOPA2 (trace (ii)) with the noise level of a regular FOPA, which is represented by trace (vi), one sees although the noise of the signal/idler input of the FOPA2 with correlated inputs (trace v) is higher than that of the regular FOPA (the same as SNL of trace (i)), the noise of FOPA2 is about 1 dB lower than the regular FOPA due to the noise cancellation induced by the correlated inputs.

Comparing Figs. 4(a) and 4(b), one sees that the noise performances measured at the signal and idler output ports are very similar. However, there are two obvious differences between them. First, under the same experiment condition, the measured noise level in Fig. 4(b) is higher than that in Fig. 4(a) because the power of LOi is about 5 times higher than that of LOs. Second, the difference between the maximum and the minimum values of trace (ii) in Fig. 4(b) is greater than that in Fig. 4(a). We think this is very likely due to the difference between the mode matching efficiencies of HDs and HDi. In the experiment, the total detection efficiencies at both the signal and

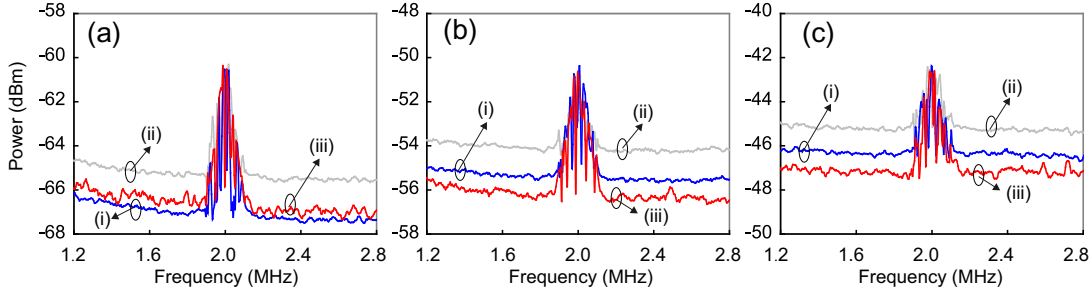


Figure 5. (a) The SNR of the input signal of FOPA2 obtained by blocking the pump of P2; (b) and (c) are the SNRs at the signal and idler output ports of FOPA2, respectively. Traces (i) are obtained by blocking the pump P1, which correspond to the SNRs of the regular amplifier; traces (ii) are obtained by blocking the idler input port of FOPA2, which correspond to the SNRs of the amplifier having the vacuum and signal with thermal noise in the idler and signal input ports, respectively; and traces (iii) are obtained by launching the correlated signal and idler fields into FOPA2, which correspond to the SNRs of the amplifier with correlated inputs. Particularly in plot (a), trace (iii) are obtained by subtracting measured idler input noise from trace (ii) with a radio frequency subtractor.

idler output ports are 48% when the transmission efficiency of about 70% between the output end of DSF1 and the input end of DSF2, the transmission efficiency of about 80% between the output end of DSF2 and the input end of HDs/HDi, and the detection efficiency of about 85% for both HDs and HDi are included. But the temporal mode matching efficiencies of HDs and HDi, which is estimated by injecting the coherent input $|\alpha\rangle$, blocking P1, and measuring the visibility of interference between the LOs/LOi and the amplified signal/idler, are about 72% and 84%, respectively. Therefore, for the result of traces (ii), improving the temporal mode matching of HDs/HDi might increase the difference between the measured maximum and minimum noise levels.

It is worth noting that we also study the noise performance of FOPA2 by varying the power levels of P1 and P2. The results show that we can not observe the noise cancellaiton effect when the pump P1/P2 is greater/lower than 1.2/1.5 mW. However, when the pump powers of P1 and P2 are respectively within the ranges of 0.6-1.1 and 1.5-2 mW, obvious noise cancellation can always be obtained. This experimental observation is different from the theoretical prediction (see Eq. (10)): best noise cancellation is obtained for $\mu_1 = \mu_2, \nu_1 = \nu_2$, i.e., FOPA2 is a reverse process of FOPA1. The reason which leads to the deviation between theory and experiment is currently unclear yet.

3.3. Low noise amplification

We then study the NF of FOPA2. In the experiment, the powers of the pumps P1 and P2 are still fixed at 1.1 and 1.7 mW, respectively, and the power of the weak probe light propagating through the EOM is 2 nW. The information encoded on the EOM, which is a sinusoidal modulation signal with the frequency of 2 MHz, is amplified by FOPA2. We first characterize the NF by measuring the SNRs at the input and output

Table 1. The signal to noise ratio (SNR) and noise figure (NF) of FOPA2 in different cases

	FOPA2 with P1 blocked ($\mu_1 = 1, \nu_1 = 0$)	FOPA2 with idler input blocked	FOPA2 with correlated inputs
SNR	$R_{in}^{(v)} = 6.69 \pm 0.05\text{dB}$ $R_s^{(v)} = 5.14 \pm 0.05\text{dB}$ $R_i^{(v)} = 3.94 \pm 0.04\text{dB}$	$R_{in}^{(th)} = 4.93 \pm 0.04\text{dB}$ $R_s^{(th)} = 3.42 \pm 0.05\text{dB}$ $R_i^{(th)} = 2.23 \pm 0.07\text{dB}$	$R_{in}^{(c)} = 6.49 \pm 0.05\text{dB}$ $R_s^{(c)} = 5.64 \pm 0.05\text{dB}$ $R_i^{(c)} = 4.58 \pm 0.05\text{dB}$
NF	$N_s^{(v)} = 1.55 \pm 0.07\text{dB}$ $N_i^{(v)} = 2.75 \pm 0.07\text{dB}$	$N_s^{(th)} = 1.51 \pm 0.08\text{dB}$ $N_i^{(th)} = 2.70 \pm 0.07\text{dB}$	$N_s^{(c)} = 0.85 \pm 0.08\text{dB}$ $N_i^{(c)} = 1.91 \pm 0.07\text{dB}$

ports of the FOPA2 with correlated inputs when the phase of P2 is fixed at the point to achieve the lowest noise. To illustrate the NF improvement, we also carry out the same measurement procedure in the following two cases: (i) the pump P1 is blocked ($\mu_1 = 1, \nu_1 = 0$), and (ii) idler input port of FOPA2 is blocked. In case (i), FOPA2 function as a regular amplifier, and the noise of input signal corresponds to SNL because the 2 nW probe is solely obtained by heavily attenuating the light spectrally carved from the fiber laser. In case (ii), FOPA2 functions as a amplifier having the vacuum and signal with thermal noise in the idler and signal input ports, respectively. The results are shown in Fig.5, in which the traces labeled "(iii)" correspond to the measurement for FOPA2 with correlated inputs, while the traces labeled "(i)" and "(ii)" correspond to the measurement for cases (i) and (ii), respectively. For convenience, we summarize and list the SNRs and NFs presented in Fig.5 in Table I.

Figure 5(a) shows the SNRs of the input signal of FOPA2 in different cases. During the measurement, the pump P2 is blocked ($\mu_2 = 1, \nu_2 = 0$). One sees that heights of the modulated signal in three traces are almost the same, but their noise levels are different. The SNR of each trace is obtained by firstly linear fitting the noise level with the data in the frequency range of 1.2-1.9MHz and 2.1-2.8MHz, and then calculating the difference between the maximum point of the trace and the linear fitting. The noise level of trace (i) is equivalent to trace (i) in Fig. 4(a). We find that the SNR of the input signal of a regular amplifier is $R_{in}^v = 6.69 \pm 0.05$ dB. The noise level of trace (ii), equivalent to the trace (v) in Fig. 4(a), is about 2 dB higher than that of trace (i) because the individual signal field out of FOPA1 is of thermal nature. So the SNR of the amplifier having the vacuum and signal with thermal noise in the idler and signal input ports becomes $R_{in}^{th} = 4.93 \pm 0.04$ dB. The noise level of trace (iii), obtained by subtracting measured correlated idler input noise from trace (ii) of Fig. 5(a) with a radio frequency subtracter, is about 1.5 dB lower than that of trace (ii). Comparing traces (ii) and (iii), it is clear that the presence of the correlated idler field improves the SNR from $R_{in}^{th} = 4.93 \pm 0.04$ dB to $R_{in}^c = 6.49 \pm 0.05$ dB. We note that according to the theoretical analysis, the level of trace (iii) should be lower than that of trace (i) due to the noise cancellation effect, however, in our experiment, trace (iii) is slightly higher than trace (i). We believe this is because the transmission efficiency between DSF1 and DSF2 is

Noise figure improvement and quantum information tapping in a fiber optical parametric amplifier with correlated inputs
currently not high enough.

Figure 5(b) [5(c)] demonstrates the SNRs of the amplified signal at the signal [idler] output port. Using the results in Figs. 5(b) [5(c)] and 5(a), the NF of the amplifier at signal [idler] output port in different cases can be consequently deduced. From trace (i), whose noise level corresponds to trace (vi) in Fig. 4(a) [4(b)], we find the SNR is $R_s^v = 5.14 \pm 0.04$ [$R_i^v = 3.94$] dB. So the NF of the regular amplifier at the signal [idler] port is $N_s^v = R_{in}^v/R_s^v = 1.55$ [$N_i^v = 2.75$] dB. For trace (ii), whose noise level corresponds to trace (iv) in Fig. 4(a) [4(b)], the SNR is $R_s^{th} = 3.42 \pm 0.05$ [$R_i^{th} = 2.23 \pm 0.07$] dB. So the NF of the FOPA2 with idler input port blocked is $N_s^{th} = 1.51 \pm 0.08$ [$N_i^{th} = 2.70 \pm 0.07$] dB, which is about the same as that of a regular amplifier. Trace (iii), whose noise level corresponds to trace (iii) in Fig. 4(a) [4(b)], shows the SNR of FOPA2 with correlated input is $R_s^c = 5.64 \pm 0.05$ [$R_i^c = 4.58 \pm 0.05$] dB, leading to a NF of $N_s^c = 0.85 \pm 0.08$ [$N_i^v/N_i^c = 1.91 \pm 0.07$] dB, which is better than that of the regular amplifier.

We compare the results of traces (i) and traces (iii) in Fig. 5 and find that the improvement of the NF due to the noise cancelation of correlated inputs is $N_s^v/N_s^c = 0.7 \pm 0.10$ [$N_i^v/N_i^c = 0.84 \pm 0.09$] dB. The improvement of NF implies our amplification scheme is suitable for amplifying the information carried by weak optical signals.

Moreover, for the FOPA2 with the correlated signal and idler inputs, we also consider the information transfer efficiencies of signal and idler (tap) port $T_{sig,tap}$. We find $T_{sig} = R_s^c/R_{in}^c = 5.69 - 6.48 = -0.81dB = 0.83$ and $T_{tap} = R_i^c/R_{in}^c = 4.58 - 6.49 = -1.91dB = 0.64$. Hence, we have $T_{sig} + T_{tap} = 1.47 \pm 0.2 > 1$. Since the limit for any classical information tap is 1, we therefore realized a quantum information tap in the two outputs of the amplifier coupled to the correlated sources.

4. Summary

In summary, we have built a low noise FOPA with correlated input. Comparing with a regular FOPA with vacuum in the unused idler input port, the noise level of the low noise FOPA is reduced about 1 dB in both the signal and the idler output channels, so that the SNR is increased accordingly when the FOPA is used in the amplification of weak signal measurement. We also measured the noise figures for the FOPA with correlated input and compared with a regular FOPA. An improvement of 0.7 ± 0.10 and 0.84 ± 0.09 dB is observed from the signal and idler outputs, respectively. These results show that our amplification scheme is suitable for the application of high precision measurement with weak input signals. Moreover, when the low noise FOPA functions as an information splitter, the device has a total information transfer efficiency of $T_{sig} + T_{tap} = 1.47$, which is greater than the classical limit of one. We therefore have achieved a quantum information tap as well. Furthermore, the experimental results are currently not as good as the theoretical predictions, because the noise reduction in our system is limited by the optical losses between two FOPAs [23], by the imperfect temporal mode-matching, and by the excess noise of the fiber laser. We believe the performance of the low noise FOPA could be further enhanced once these factors are technically taken care of.

This work was supported in part by the State Key Development Program for Basic Research of China (No. 2014CB340103), the Specialized Research Fund for the Doctoral Program of Higher Education of China (No. 20120032110055), the National Natural Science Foundation of China (No. 11304222) and 111 Project B07014.

References

- [1] W. H. Louisell, *Coupled Mode and Parametric Electronics* (Wiley, New York, 1960); *Radiation and Noise in Quantum Electronics* (McGraw-Hill, New York, 1964).
- [2] C. M. Caves, Phys. Rev. D **26**, 1817 (1982).
- [3] H. P. Yuen, Phys. Rev. Lett. **56**, 2176 (1986).
- [4] J. A. Levenson, I. Abram, Th. Rivera, and P. Grangier, J. Opt. Soc. Am. B **10**, 2233 (1993).
- [5] S. K. Choi, M. Vasilyev, P. Kumar, Phys. Rev. Lett. **83**, 1938 (1999).
- [6] Z. Tong, C. Lundström, P. A. Andrekson, C. J. McKinstrie, M. Karlsson, D. J. Blessing, E. Tipsuwannakul, B. J. Puttnam, H. Toda, and L. Grüner-Nielsen, Nat. Photon. **5**, 430 (2011).
- [7] R. J. Mears, L. I. Reekie, M. Jauncey, and D. N. Payne, Electron. Lett. **23**, 1026 (1987).
- [8] M. N. Islam, IEEE J. Sel. Top. Quantum Electron. **8**, 548 (2002).
- [9] G. J. Milburn, M. L. Steyn-Ross, and D. F. Walls, Phys. Rev. A **35**, 4443 (1987).
- [10] Z. Y. Ou, S. F. Pereira, and H. J. Kimble, Phys. Rev. Lett. **70**, 3239 (1993).
- [11] Z. Y. Ou, Phys. Rev. A **48**, R1761–R1764 (1993).
- [12] J. Kong, F. Hudelist, Z. Y. Ou, and W. Zhang, Phys. Rev. Lett. **111**, 033608 (2013).
- [13] J. H. Shapiro, Opt. Lett. **5**, 351 (1980).
- [14] J. A. Levenson, I. Abram, T. Rivera, P. Fayolle, J. C. Garreau, and P. Grangier, Phys. Rev. Lett. **70**, 267 (1993).
- [15] J. P. Poizat and P. Grangier, Phys. Rev. Lett. **70**, 271 (1993).
- [16] S. F. Pereira, Z. Y. Ou, and H. J. Kimble, Phys. Rev. Lett. **72**, 214 (1994).
- [17] Hai Wang, Yun Zhang, Qing Pan, Hong Su, A. Porzio, Changde Xie, and Kunchi Peng, Phys. Rev. Lett. **82** 1414 (1999).
- [18] Z. Y. Ou, S. F. Pereira, H. J. Kimble and K. C. Peng, Phys. Rev. Lett. **68**, 3663 (1992).
- [19] E. Flurin, N. Roch, F. Mallet, M. Devoret, and B. Huard, Phys. Rev. Lett. **109**, 183901 (2012).
- [20] Z. Y. Ou, Phys. Rev. A **85**, 023815 (2012).
- [21] J. Jing, C. Liu, Z. Zhou, Z. Y. Ou, and W. Zhang, Appl. Phys. Lett. **99**, 011110 (2011).
- [22] X. Guo, X. Li, N. Liu, L. Yang, and Z. Y. Ou, Appl. Phys. Lett. **101**, 261111 (2012)
- [23] A. M. Marino, N. V. Corzo Trejo, and P. D. Lett, Phys. Rev. A **86**, 023844 (2012).